

HIGH TEMPERATURE PROCESSING OF FLY ASH FOR THE PRODUCTION OF AN ENVIRONMENTALLY SAFE MATERIAL

Zaid Ghouleh¹, M. Isac², R.I.L.Guthrie³, P. Carabin⁴

¹ M.Eng Candidate, McGill University, zaid.ghouleh@mcgill.ca

² Research Manager, McGill Metals Processing Centre (MMPC), mihaiela.isac@mcgill.ca

³ Director, McGill Metals Processing Centre (MMPC), rod@mmpc.mcgill.ca

McGill University, McGill Metals Processing Centre (MMPC)
3610 University Street, Montreal, Canada, H3A 2B2
Phone: (514) 398-1555

⁴ Chief Engineer, PyroGenesis Canada Inc., pcarabin@pyrogenesis.com

PyroGenesis Canada Inc.
1744 Williams, Suite 200, Montreal, Quebec, Canada, H3J 1R4
Phone: (514) 937-0002 ext. 274, Fax: (514) 937-5757

ABSTRACT

The primary goal of this research was to devise a process to treat hazardous fly ash, so as to render it environmentally stable and useful for industrial, structural, and ornamental applications. The process selected, entails transforming fly ash into a glass-ceramic material. The technique adopted was to melt the fly ash into a slag, to hold it at 1500°C for 2 hours, followed by water quenching. The amorphous products obtained were then heat treated, so as to nucleate and crystallize parts of the material. The specific heat treatment devised was based on results obtained from thermal analysis: nucleation was carried out at 805°C for 60min, followed by two crystallization events at 905°C and 990°C, respectively, each lasting for 30min. Material characterization and chemical analysis were carried out with the help of XRF, XRD, TCLP, SEM/EDS, DTA, TMA, Optical Microscopy, Confocal Laser Microscopy, and Vickers micro-hardness. The final product obtained was a glass-ceramic material with randomly oriented crystals embedded in its residual amorphous matrix. The crystalline phases forming were identified as Nepheline and Diopside. Leaching test results revealed a significant reduction in heavy metal release. Values obtained from mechanical testing showed that the fly-ash derived glass-ceramic material had increased hardness (830HV vs. 650HV) and strength compared to its amorphous parent material.

INTRODUCTION

Humanity's current trends in consumption are leading to unprecedented levels of waste products. The United Nations and other agencies estimate that the current production of municipal solid waste (MSW), worldwide, ranges between 1 and 1.3 billion tonnes per year [1]. While Canada is not one of the top producers of MSW, accounting for only 12 million tonnes in 2005, this amount is relatively high with an annual average production of 302kg per citizen [2].

The environmental concern with MSW production is that only a small fraction of these wastes is successfully recycled or diverted from landfills. In 2005, Canada deposited 79% of its MSW into landfills [2]. However, although the practice of landfilling is inexpensive and practical, it has serious environmental repercussions. It can also involve occupying vast stretches of land, difficult for regions of high population density and limited disposal spaces. Increased environmental awareness and geographic challenges pose serious constraints for this practice.

Incineration is an alternative mode of waste handling, and an effective one. It is a widely implemented method that entails the thermal combustion of MSW. One of the main benefits of this process is that it is capable of substantially reducing waste volume, by up to 90% [3, 4]. Environmentally, it resolves problems of odoriferous emissions and leachate seepage associated with conventional landfilling [3]. On the downside, however, it generates unstable residues of bottom ash, and fly ash. The amount of bottom ash and fly ash produced is equivalent to approximately one third the initial weight of MSW burned. Bottom ash consists of a clinker type of material that accumulates at the bottom of the incinerator, hence its name. The finer fly ash is carried with the exhaust flue gas, and is later collected by air pollution control devices downstream. Conventionally, these residues are disposed of in landfills.

Of the two ash types, fly ash is regarded as the more toxic due to its constituents. When landfilled, it can inflict adverse ecological and environmental effects. "[It's] management [is] one of the most important environmental issues related to the incineration of MSW [5]." It contains high levels of leachable heavy metals, toxic organic contaminants such as dioxins, furans, Poly-Aromatic Hydrocarbons (PAHs), and Volatile Organic Compounds (VOCs) [5, 6]. Increased environmental awareness has led a number of countries prohibiting the landfilling of untreated fly ash. As a result, fly ash is required to undergo treatments to render it environmentally stable prior to its disposal.

Vitrification is one of the most promising inertisation techniques since it achieves effective containment of the fly ash's toxic constituents. It involves the conversion of fly ash into an amorphous material. By doing so, it rids the fly ash of 99.9% of its hazardous organic constituents and fixes the heavy metals in the final glass-like product [7, 8]. Its composition largely comprises SiO_2 , Al_2O_3 , and CaO . In fact, MSW fly ash typically falls within the margins of the $\text{CaO-Al}_2\text{O}_3\text{-SiO}_2$ ternary glass system shown in Figure 1 (the black dot in the diagram locates the fly ash used in this study). The fly ash's glass-forming constituents will ensure that an amorphous material is obtained upon melting and subsequent rapid cooling. This material is stable and leach resistant, hence, it can be safely disposed of in landfills, or used as raw materials for certain relevant applications [3, 8]. Not only is vitrification an effective stabilizing technique, it also achieves further volume reduction, reportedly, a third to a half of the original quantity [8].

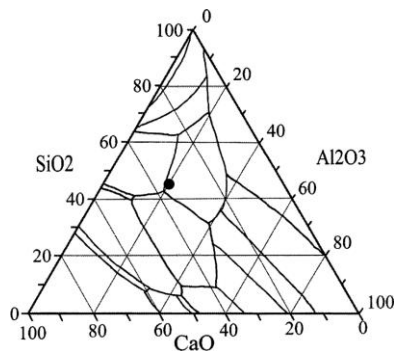


Figure 1: CAS (CaO-Al₂O₃-SiO₂) ternary phase diagram.

The effectiveness of vitrification as a treatment for stabilizing fly ash is inarguable. However, the same cannot be said concerning its use as a practical raw material. It has been a rising debate whether these vitreous products have sufficient mechanical characteristics that would allow their safe use. Different regional regulations and restrictions make reaching a worldwide consensus on accepted uses difficult to achieve. Individual studies by Nishida and Boccaccini deem these products unsuitable for use in civil engineering works [9, 10]. These products have limited applications and are normally landfilled with no economic benefit. Moreover, vitrification can prove to be costly since it is an energy-intensive process. High energy consumption can be justified if a value-added product with high market value can be produced, thereby offsetting the costs of fabrication. As some studies have demonstrated, this can be achieved by converting vitreous products into glass-ceramics by means of carrying out controlled heat treatments [7, 11].

Converting vitreous fly ash into a glass-ceramic can be achieved via a two-step heat treatment that induces both nucleation and crystallization. The outcome is a material with randomly oriented crystals embedded in a residual glass matrix. Nucleation is the first step and it involves the formation of stable nuclei within the glass matrix. The subsequent crystallization step, carried out at a higher temperature, promotes crystal growth and the formation of a new crystalline phase [11]. The chemical composition of fly ash makes pursuing the production of glass-ceramics feasible, and the subject of much ongoing research. Glass-ceramics, in general, are known to exhibit high mechanical strength, good dimensional stability, superior chemical durability, and notable abrasion resistance [12]. The processing route and the type of glass-ceramic sought, are highly dependant on the composition of the initial fly ash.

METHODOLOGY

The fly ash used in this research study was supplied by the Quebec City Municipal Waste Incinerator. The chemical composition was determined from XRF analysis performed using a PANalytical PW2440 spectrometer (MagiX PRO series). Sulfur and carbon contents were measured by means of an ELTRA CS-800 Carbon/Sulfur analyzer. Loss on Ignition (LOI) was measured in accordance with ASTM standards. TCLP was also performed on the fly ash as prescribed by US EPA Method 1311. The crucibles used for melting the fly ash were machined from refractory bricks comprised of 83%Al₂O₃-11%Cr₂O₃-2%SiO₂. After being compacted into the crucible, the fly ash was heated to 1500°C and held at that temperature for 2 hours to ensure homogenous melting. The resulting slag was then quenched in water at room temperature to form a black vitreous material with irregular dimensional shapes. This pebble-sized material was then dried and divided into two

batches. The first batch was intended for undergoing analytical tests while the second was kept aside for pursuant heat treatments.

From the first batch, a portion of the vitreous product was pulverized to undergo X-Ray Diffraction (XRD), Differential Thermal Analysis (DTA), and Thermo-Mechanical Analysis (TMA). XRD was performed using a Philips PW-1050/65 machine with a 2θ scan range between 10° and 100° at a step size of 0.02° and scan step time of 2 seconds. A PERKIN ELMER DTA-7 was used for the DTA test that spanned from room temperature to 1350°C at a rate of $10^\circ\text{C}/\text{min}$. TMA was carried out using a TA TMA-Q400 that was set to achieve a final temperature of 950°C at a heating rate of $5^\circ\text{C}/\text{min}$.

Additional appraisal tests performed on the vitreous samples include leaching and micro-hardness. Vickers micro-hardness was carried out using a CM-100AT Clark Micro-hardness Tester with a load of 100g and an indentation time of 10 seconds. Similar to the fly ash, the leaching procedure adopted for the vitreous product was US EPA Method 1311.

Based on the DTA results obtained, a four step heat treatment procedure was devised for the conversion of the vitreous material into a glass-ceramic. The glass-ceramic product correspondingly was submitted to XRD, TCLP, TMA, and micro-hardness, tests.

Micro-structures and phase transformations, were studied using Optical Microscopy, Scanning Electron Microscopy (SEM), and Confocal Laser Scanning Microscopy (CLSM). As-produced glass-ceramic samples were mounted and polished prior to characterization. Optical microscopy was performed using a Leica DM-IRM microscope with Clemex image analyzer software. Similarly, SEM characterization was conducted on a Philips XL30 FESEM operating at an accelerating voltage of 15kV. This analysis necessitated that the samples be coated with a thin layer of Au-Pd to make them conductive, and etched in a 5% HF solution for 30 seconds. The laser confocal microscope used was a Lasertec 1LM21-SVF17SP that allows ultra high temperature *in-situ* observation, and real-time recording.

All vitrification and devitrification heat treatments were carried out in a Thermolyne F46240CM furnace under atmospheric conditions.

RESULTS AND DISCUSSION

Fly Ash Composition and Loss on Ignition (LOI)

The composition of the fly ash as determined from XRF is presented in Table 1. Major components are listed in their most probable oxide form in weight %, while trace components are expressed in their elemental form. As expected, the main constituents are SiO_2 , Al_2O_3 , and CaO , combine to make up approximately 63% of the total composition. The LOI value obtained for the fly ash was 7.12%. This loss in weight was attributed to the vaporization of moisture and/or chlorine, and the oxidation of carbon and sulfur.

Table 1: Composition of MSW incinerator fly ash

Oxides	Weight %	Elements	ppm
SiO_2	28.86	Ag	426
TiO_2	2.53	Ba	2213
Al_2O_3	11.73	Br	1214
Fe_2O_3	5.62	Cr	431
MnO	0.11	Cu	1078

MgO	2.96	F	4131
CaO	22.03	Ni	176
Na ₂ O	4.48	Pb	1702
K ₂ O	3.30	Sb	1850
P ₂ O ₅	4.55	Sn	664
Cl	4.62	Sr	460
S	2.25	Zn	9470
C	4.43	Zr	221

Thermo-Mechanical Analysis (TMA)

The vitrification of the fly ash yields a black amorphous material referred to, in this study, as the “vitreous” sample. TMA was performed on this sample to determine its coefficient of thermal expansion (CTE) and, also, to acquire more insight on its sintering behavior. The shrinking in length of the pelletized sample commenced at 724°C and persisted up to a temperature of 910°C. This shrinkage illustrates the dimensional change experienced as a result of sintering, which also occurs on the account of the decreasing viscosity. It is within this temperature range that the optimum sintering temperature can be found. As a result, the total reduction in length was 7.62%, or 0.664mm from its initial value of 8.718mm. Moreover, the CTE for the vitreous material was calculated to equal 8.32 $\mu\text{m}/\text{m}\cdot^{\circ}\text{C}$ (50-700°C). Similarly, a slightly lower value of 7.87 $\mu\text{m}/\text{m}\cdot^{\circ}\text{C}$ (50-700°C) was obtained for the produced glass-ceramic material. This lower value implies that, with increasing temperatures, the glass-ceramic material will experience a relatively smaller dimensional change than the vitreous material. Ceramics and glasses are known to exhibit small CTE's, typically between 0.5 $\mu\text{m}/\text{m}\cdot^{\circ}\text{C}$ and 15 $\mu\text{m}/\text{m}\cdot^{\circ}\text{C}$ [13]. For such material, a low CTE is a desirable quality, for it is a measure of potential resistance to thermal shock.

Thermal Analysis

The behavior of the vitreous sample during thermal analysis can be seen in the DTA plot shown in Figure 2. Furthermore, the findings are summarized in Table 2. The first apparent feature on the heat curve is that of a shallow endothermic dip with an onset temperature of 730°C. This onset temperature is ascribed to glass transition, T_g. The second small endothermic dip occurs at around 800°C and, based on similar research by T.W. Cheng, is identified as the dilatometric softening point [14]. Two subsequent exothermic peaks, both denoting crystallization, occur at 893°C and 977°C. The first crystallization peak is smaller and much less pronounced than the second. Both these peaks imply physical changes in the sample, or more precisely, the formation of new crystalline phases. Melting appears as a notable endothermic decline, where the total melting of the sample is achieved by 1181°C.

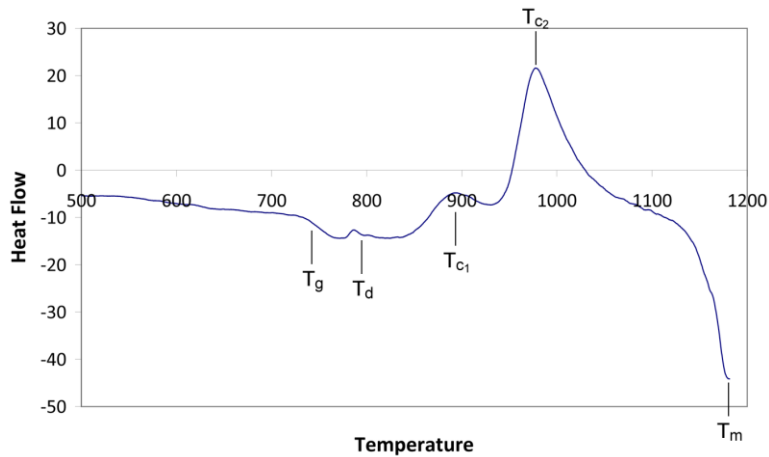


Figure 2: DTA heat curve for the vitreous sample

Table 2: Summary of DTA results for vitreous sample

Thermal activity	Symbol	Temperature (°C)
Glass Transition Temperature	T _g	730
Dilatometric Softening Point	T _d	793
Crystallization Temperature 1	T _{c1}	893
Crystallization Temperature 2	T _{c2}	977
Melting Temperature	T _M	1181

Preparing Glass-Ceramic Material

From DTA findings, a heat treatment schedule was devised. This four step heat treatment is presented in Figure 3. The selection of the steps was based on the premise that the mechanisms of nucleation and crystallization are prompted by holding the vitreous material at least 10°C above its respective glass transition and crystallization temperatures [15]. The heat treatment included the nucleation step at 805°C for 60 minutes to form stable nuclei within the amorphous matrix, two crystallization steps at 905°C and 990°C, respectively, each lasting 30 minutes, and finally an annealing step at 600°C for 45 minutes to relieve internal thermal stresses.

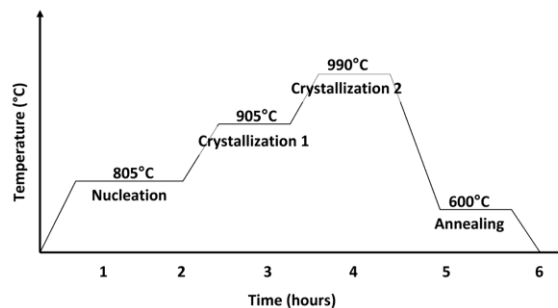


Figure 3: Heat treatment devised for the production of a glass-ceramic material

X-Ray Diffraction Analysis

XRD analysis was performed on the glass-ceramic material produced. The results are presented in Figure 4. Thorough pattern matching with the aid of PANalytical X'Pert HighScore software, identified Nepheline and Diopside as the main crystalline phases present in the final product. Matching peaks have a slight variation in intensities due to diffraction interferences and overlapping caused from the complex nature of the compounds that form. In order to determine which phase grows first, an additional XRD analysis was performed on the vitreous product after it had only completed the first crystallization step. The resultant spectrum is shown in Figure 5, and pattern matching identifies it as belonging to the Nepheline phase. Hence, the first crystallization peak T_{c1} observed in the DTA heat curve involves the formation of the Nepheline phase, while T_{c2} involves that of the Diopside phase. The identified variants of Nepheline and Diopside have the chemical formulas $\text{Na}_{2.8}\text{K}_{0.6}\text{Ca}_{0.2}\text{Al}_{3.8}\text{Si}_{4.2}\text{O}_{16}$ and $\text{Ca}(\text{Mg}, \text{Al})(\text{Si}, \text{Al})_2\text{O}_6$, respectively.

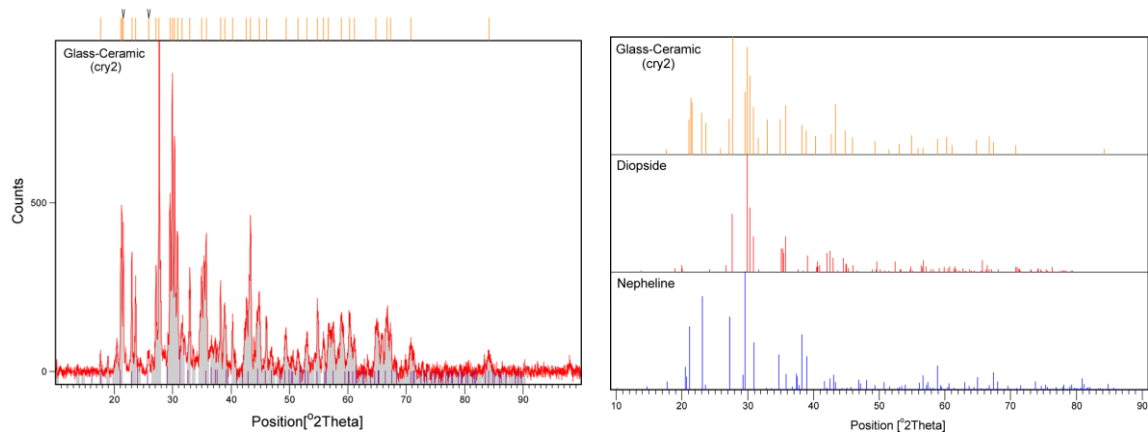


Figure 4: XRD spectrum for the vitreous sample after completing the heat treatment

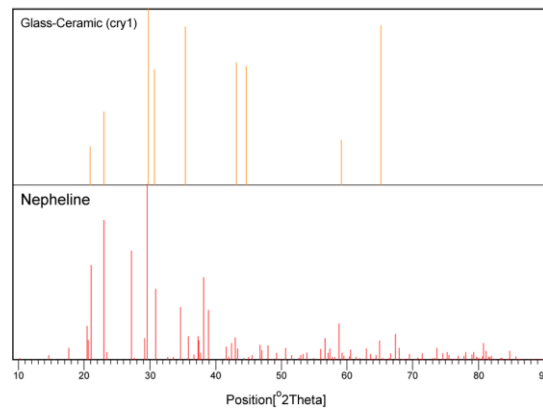


Figure 5: XRD peak matching for the vitreous sample after being heat treated at 805°C for 60min and 905°C for 30min.

Microstructure Analysis

Of the different techniques employed for surface characterization, SEM provided the most significant information on the micro-structure of the sample. Moreover, it is in agreement with the previous XRD findings. Scanning the sample using an optical microscope did not reveal distinct features for reasons of opacity and light reflection caused from the residual glass phase. The confocal laser microscope was used for the purpose of observing micro-structural changes that occur in the vitreous sample as it is being heated. However, the dark nature of the vitreous sample posed constraints on visibility, especially at higher magnifications. Nonetheless, minute changes in the microstructure were faintly observed with increasing temperature and holding times. Data acquisition was in the form of continuous live feed recording, difficult to reproduce effectively as snapshot frames.

SEM micrographs for the glass-ceramic material at different magnifications are shown in Figure 6. The darker regions in Figure 6(a) are chasm-like depressions that were once occupied by an amorphous phase prior to being dissolved by the HF etchant. The bright regions are those of the Nepheline phase. In the literature, Nepheline is identified as having a hexagonal crystal structure. Figure 6(b) is taken at a higher magnification and, in addition to Nepheline, it also reveals the presence of the second crystalline phase, Diopside. The Diopside phase forms at a higher temperature, and is notably smaller in size. These crystals stretch a couple of microns in length as opposed to the Nepheline crystals, which can extend to more than 20 microns.

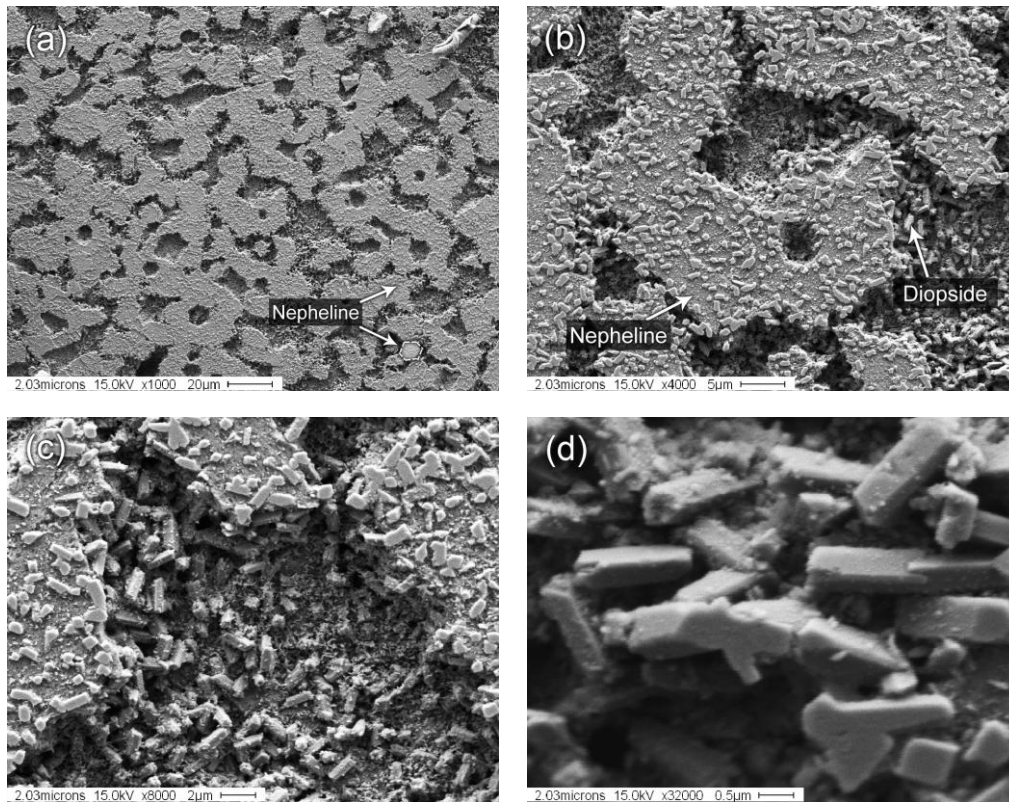


Figure 6: SEM micrographs of the produced glass-ceramic material at different magnifications showing crystals of hexagonal Nepheline and monoclinic Diopside: (a) x1000, (b) x4000, (c) x8000, and (d) x32000.

The small depositions seen covering the surface of the Nepheline crystals are, in fact, remnants of the Diopside phase that had been sliced off during polishing. Figures 6 (c) and (d) are close up images of the Diopside crystals. As shown, and complemented by the literature, these pillar-like crystals have a monoclinic structure, better described as rectangular prisms with parallelograms as their bases.

Vickers Micro-Hardness

For comparison, micro-hardness was performed on both the vitreous and the glass-ceramic material. The results are summarized in Table 4. As revealed, there is a considerable increase in hardness upon transforming the vitreous material into a glass-ceramic. This is also met by an increase in toughness noted from increased rigidity and reduced brittleness when manually handling the samples. This increase in hardness is owed to the crystalline phases that form. In fact, related studies note that the presence of Diopside in the glass-ceramic significantly improves mechanical properties pertaining to hardness and strength [16]. The standard deviation for the glass-ceramic sample is notably higher than that of the vitreous one. This is a result of the glass ceramic's inhomogeneous surface since it is comprised of randomly oriented crystals within an amorphous matrix. In contrast, the surface of the vitreous sample is relatively homogenous throughout.

Table 3: Average Vickers hardness values for the vitreous and glass-ceramic samples

	Micro-hardness (HV)
Vitreous	648.2 ± 6.3
Glass-ceramic	824.3 ± 32.2

Heavy Metal Leaching

The leaching performances of the fly ash, the vitreous material, and the glass-ceramic product, were all evaluated using US EPA TCLP Method 1311. AAS results for the concentration of toxic heavy metals that leach into solution are presented in Table 5. As expected, the vitrification of the fly ash yielded excellent leaching results. The amounts of heavy metals that leach from the vitreous material are almost negligible when compared to the results obtained for the pure fly ash. The heavy metals become encapsulated within the amorphous structure and, hence, the product is rendered inert. Likewise, the glass-ceramic material also demonstrates superior resistance to leaching. As can be seen, its performance is even slightly better than that of its parent vitreous material. In the glass-ceramic, the heavy metals effectively replace Al^{3+} and Ca^{2+} ions present in the silicate matrix [8]. The released ions then become incorporated in the make-up of the crystalline phases that form. Similar research by Park and Piscicella describe that the enhanced chemical stability of their produced glass-ceramics is owed to the Diopside's stable interlocking crystal structure [16, 17].

Table 4: TCLP results for Fly Ash, Vitreous material, and Glass-ceramic product

	Concentration: ppm (mg/L); Detection Limit (DL) = 0.001 ppm		
	Fly Ash	Vitreous	Glass-ceramic
Cr	1.406	< DL	0.039
Cu	13.590	1.291	0.486
Pb	18.000	0.580	0.200
Zn	133.100	1.022	0.198
Cd	1.130	< DL	< DL

CONCLUSIONS

This study demonstrates the successful treatment and conversion of toxic MSW fly ash into a glass-ceramic material. XRD analysis identified the crystalline phases that form to be Nepheline and Diopside. These findings were complemented by the DTA and SEM examinations. The final product obtained, is a (Nepheline/Diopside)-based glass-ceramic. Leaching and mechanical tests show this material to be environmentally stable and fit for use in structural and ornamental applications.

ACKNOWLEDGEMENTS

The authors would like to acknowledge the financial support of NSERC and BIOCAP, and the technical assistance of Dr. Janusz A. Kozinski, Dean and Professor, College of Engineering, University of Saskatchewan, and Dr. Lakshminarayana Rao, Product Development Scientist, PyroGenesis Canada Inc.

REFERENCES

1. Malone, R. *Garbage: World's Worst Waste*. Forbes 2006 [cited May 24, 2006]; Available from: http://www.forbes.com/logistics/2006/05/23/waste-worlds-worst-cx_rm_0524waste.html.
2. Statistics Canada (2005) *Human Activity and the Environment: Annual Statistics 2005*. **Volume**,
3. Park, Y.J. and J. Heo, *Vitrification of fly ash from municipal solid waste incinerator*. Journal of Hazardous Materials, 2002. **91**(1-3): p. 83-93.
4. Ilex Energy Consulting, *Eligibility of Energy from Waste - Study and Analysis*, S.o.S.f.T.a. Industry, Editor. 2005: UK.
5. Ferreira, C., A. Ribeiro, and L. Ottosen, *Possible applications for municipal solid waste fly ash*. Journal of Hazardous Materials, 2003. **96**(2-3): p. 201-216.
6. Millrath, K. and N.J. Themelis. *Waste as a Renewable Source of Energy: Current and Future Practices*. in *ASME International Mechanical Engineering Congress & Exposition (IMECE)*. 2003. Washington D.C.
7. Rincó, J.M., M. Romero, and A.R. Boccaccini, *Microstructural characterisation of a glass and a glass-ceramic obtained from municipal incinerator fly ash*. Journal of Materials Science, 1999. **34**(18): p. 4413-4423.
8. Cheng, T.W., *Effect of additional materials on the properties of glass-ceramic produced from incinerator fly ashes*. Chemosphere, 2004. **56**(2): p. 127-131.
9. Boccaccini, A., Dr. and R. Rawlings, Prof, *Glass-Ceramics from Waste Materials*. Materials World, 2002. **10**(2002): p. 16-18.
10. Nishida, K., et al., *Melting and Stone Production Using MSW Incinerated Ash*. Waste Management, 2000. **21**(no: 5 (3 ref.)): p. 443-449.
11. Erol, M., S. Kucukbayrak, and A. Ersoy-Mericboyu, *Production of glass-ceramics obtained from industrial wastes by means of controlled nucleation and crystallization*. Chemical Engineering Journal, 2007. **132**(1-3): p. 335-343.
12. Peng, F., et al., *Nano-crystal glass-ceramics obtained by crystallization of vitrified coal fly ash*. Fuel, 2004. **83**(14-15): p. 1973-1977.
13. Callister, W.D., *Materials Science and Engineering an Introduction*. Fifth ed. 2000, United States.
14. Cheng, T.W. and Y.S. Chen, *On formation of CaO-Al₂O₃-SiO₂ glass-ceramics by vitrification of incinerator fly ash*. Chemosphere, 2003. **51**(9): p. 817-824.
15. Erol, M., et al., *Characterization investigations of glass-ceramics developed from Seyitomer thermal power plant fly ash*. Journal of the European Ceramic Society, 2003. **23**(5): p. 757-763.
16. Park, Y.J., S.O. Moon, and J. Heo, *Crystalline phase control of glass ceramics obtained from sewage sludge fly ash*. Ceramics International, 2003. **29**(2): p. 223-227.
17. Piscicella, P., et al., *Chemical durability of glasses obtained by vitrification of industrial wastes*. Waste Management, 2001. **21**(1): p. 1-9.